NASA Contractor Report 187629
ICASE Report No. 91–75

ICASE

AN APPROXIMATE RIEMANN SOLVER FOR HYPERVELOCITY FLOWS

P. A. Jacobs

Contract No. NAS1–18605
September 1991

Institute for Computer Applications in Science and Engineering
NASA Langley Research Center
Hampton, Virginia 23665–5225

Operated by the Universities Space Research Association

National Aeronautics and
Space Administration

Langley Research Center
Hampton, Virginia 23665-5225

AN APPROXIMATE RIEMANN SOLVER FOR HYPERVELOCITY FLOWS

P. A. Jacobs[1]
Institute for Computer Applications in Science and Engineering
NASA Langley Research Center
Hampton, VA 23665

ABSTRACT

We describe an approximate Riemann solver for the computation of hypervelocity flows in which there are strong shocks and viscous interactions. The scheme has three stages, the first of which computes the intermediate states assuming isentropic waves. A second stage, based on the strong shock relations, may then be invoked if the pressure jump across either wave is large. The third stage interpolates the interface state from the two initial states and the intermediate states. The solver is used as part of a finite-volume code and is demonstrated on two test cases. The first is a high Mach number flow over a sphere while the second is a flow over a slender cone with an adiabatic boundary layer. In both cases the solver performs well.

[1]Research was supported by the National Aeronautics and Space Administration under NASA Contract No. NAS1-18605 while the author was in residence at the Institute for Computer Applications in Science and Engineering (ICASE), NASA Langley Research Center, Hampton, VA 23665.

Nomenclature, Units

a	: local speed of sound, m/s
E	: total energy (internal + kinetic), J/kg
e	: specific internal energy, J/kg
h	: specific enthalpy, J/kg
M	: Mach number
P	: pressure, Pa
Pr	: Prandtl number, $(C_p\mu/k)$
R	: gas constant, $J/kg/K$
Re	: Reynolds number
T	: temperature, K
t	: time, s
$\overline{U}$	: Riemann invariant
u	: x-component of velocity, m/s
v	: y-component of velocity, m/s
ws	: wave speed used in the Riemann solver
x	: x-coordinate, m
y	: y-coordinate, m
Z	: intermediate variable
α	: weighting function
ρ	: density, kg/m^3
γ	: ratio of specific heats
μ	: coefficient of viscosity, $Pa.s$

Superscripts

$*$	: intermediate states for the Riemann solver /locally tangent to the cone surface

Subscripts

MIN	: minimum allowable value
e	: boundary-layer edge condition
x,y	: cartesian components
L, R	: left state, right state

1 Introduction

In recent years the proliferation of relatively fast computers has popularized the direct calculation of viscous, compressible flows in a time-accurate manner. In some situations, such as the transient hypersonic flow over a model in a shock-tunnel, numerical simulation is the only way to extract detailed information about the flow field. Such computations are very demanding as there are both strong shocks and rarefactions and strong viscous interactions.

This note describes a robust Riemann solver for use in transient hypervelocity flow calculations. The full code [1] is based on a cell-centred time-dependent finite-volume formulation of the axisymmetric Navier-Stokes equations in which the governing equations are expressed in integral form over arbitrary quadrilateral cells. The time rate of change of conserved quantities in each cell is specified as a summation of the fluxes through the cell interfaces. The inviscid components of the fluxes are computed with the approximate Riemann solver while the viscous fluxes are calculated by application of the divergence theorem. At each time step, we first interpolate the flow state (consisting of a set of values for ρ, u, v, e, P, a) to either side of each interface at the start of the time step and then apply a Riemann solver to estimate the flow state at the interface during the time step. Note that the solver is applied in a locally rotated frame of reference in which the u-velocity is normal to the cell interface.

There are a number of Riemann solvers that can be used including "exact" iterative schemes [2] and approximate (noniterative) schemes [3, 4]. The approximate schemes are generally less computationally expensive than the iterative schemes and, because the Riemann solver comsumes a large fraction of the total computational effort, an approximate scheme is favoured. Although the Roe-type solver is popular because it is relatively fast, there are situations such as the double-Mach-reflection case [5] and flow over a sphere [6] where it may produce spurious results. The Osher-type solver [4] is considered to be fairly robust and free of adjustable parameters, however, we have experienced some difficulty in applying it to flows with very strong shocks.

Here, we take a middle road between the fully iterative solvers and the single-step approximate solver and, at the cost of some computational expense, produce an approximate solver which is reliable in extreme flow situations and is vectorizable with current compilers for vector computers.

2 Approximate Riemann Solver

The current solver is a 3-stage approximate Riemann solver in which the first stage computes the intermediate pressure and velocity assuming isentropic wave interaction. A second stage, based on the strong-shock relations, may be invoked to improve the first-stage estimate if the pressure jump across either wave are sufficiently large. In practice, this modification has been required only in extreme conditions such as those found in the bluff-body test case (Section 3.1). The final stage is to select/interpolate the interface state (ρ, u, v, e, P, etc) from the set of left, right and intermediate states. If stage 2 (strong shock modification) is not invoked, the solver is much like Osher's approximate Riemann solver [4].

STAGE 1: The first stage of the Riemann solver assumes that a spatially constant left state (subscript L) and right state (subscript R) interact through a pair of finite-amplitude (and isentropic) compression or rarefaction waves. Perfect gas relations ([7] cited in [2]) are used to obtain the intermediate states (L^*, R^*) in the gas after the passage of left-moving and right-moving waves, respectively. The expressions implemented in the code are

$$P_L^* = P_R^* = P^* = P_L \left[\frac{(\gamma - 1)(\overline{U}_L - \overline{U}_R)}{2a_L(1 + Z)} \right]^{2\gamma/(\gamma-1)} \tag{1}$$

and

$$u_L^* = u_R^* = u^* = \frac{\overline{U}_L Z + \overline{U}_R}{1 + Z} \tag{2}$$

where the Riemann invariants are

$$\begin{aligned} \overline{U}_L &= u_L + \frac{2a_L}{\gamma - 1}, \\ \overline{U}_R &= u_R - \frac{2a_R}{\gamma - 1}, \end{aligned} \tag{3}$$

and the intermediate variable Z is given by

$$Z = \frac{a_R}{a_L} \left(\frac{P_L}{P_R} \right)^{(\gamma-1)/(2\gamma)} . \tag{4}$$

Note that these expressions involve the power operator which is computationally expensive. For a limited range of base and exponent, the standard power function is replaced by the approximate expansion [1]. In the exceptional situation of $(\overline{U}_L - \overline{U}_R) < 0$, we assume that a (near) vacuum has formed at the cell interface and set all of the interface quantities to minimum values.

STAGE 2: If the pressure jump across either wave is large (say, a factor of 10), then the guess for the intermediate pressure is modified using the strong shock relations.

If $P^* > 10\ P_L$ and $P^* > 10\ P_R$ then both waves are taken to be strong shock waves and the intermediate pressure and velocity can be determined directly as

$$P^* = \frac{\gamma+1}{2}\rho_L\left[\frac{\sqrt{\rho_R}}{\sqrt{\rho_R}+\sqrt{\rho_L}}(u_L - u_R)\right]^2 \tag{5}$$

and

$$u^* = \frac{\sqrt{\rho_L}\ u_L + \sqrt{\rho_R}\ u_R}{\sqrt{\rho_R}+\sqrt{\rho_L}}\ . \tag{6}$$

If P^* is greater than P_L or P_R (but not both), the stage-1 estimate for P^* can be improved with two Newton-Raphson steps of the form

$$P^*_{n+1} = P^*_n - F_n\left(\frac{dF_n}{dP^*}\right)^{-1} \tag{7}$$

where

$$F_n = u^*_L(P^*_n) - u^*_R(P^*_n) \tag{8}$$

and

$$u^*_L = \begin{cases} \overline{U}_L - \frac{2a_L}{\gamma-1}\left(\frac{P^*}{P_L}\right)^{\frac{\gamma-1}{2\gamma}}\ , & P^* \le 10\ P_L\ , \\ u_L - \left(\frac{2P^*}{\rho_L(\gamma+1)}\right)^{1/2}\ , & P^* > 10\ P_L\ , \end{cases} \tag{9}$$

$$u^*_R = \begin{cases} \overline{U}_R + \frac{2a_R}{\gamma-1}\left(\frac{P^*}{P_R}\right)^{\frac{\gamma-1}{2\gamma}}\ , & P^* \le 10\ P_R\ , \\ u_R + \left(\frac{2P^*}{\rho_R(\gamma+1)}\right)^{1/2}\ , & P^* > 10\ P_R\ . \end{cases} \tag{10}$$

The strong-shock expressions used in (9), (10) can be obtained from the normal shock expressions in [8] by taking the limits as the pressure jump becomes large. During the update, we ensure that $P^* \ge P_{MIN}$ where P_{MIN} is some small value. After updating P^*, the intermediate velocity is evaluated using the relevant strong-shock relation from (9) or (10).

STAGE 3: Now that we have computed the pressure and velocity in the intermediate regions behind the waves, the other intermediate flow properties may be evaluated. The interface conditions used in the inviscid flux vector can then be selected or interpolated from the 4 flow states using the logic shown in Fig. 1. Note that although only the left-moving wave is discussed below, a similar procedure is used to obtain the flow state behind the right-moving wave.

If the pressure rises across the left-moving wave (i.e. $P^* > P_L$), the left wave is assumed to be a shock and density is obtained from the Rankine-Hugoniot relation as

$$\rho^*_L = \rho_L\left[\frac{(\gamma+1)P^* + (\gamma-1)P_L}{(\gamma+1)P_L + (\gamma-1)P^*}\right]\ . \tag{11}$$

The specific internal energy is obtained from the equation of state as

$$e_L^* = \frac{P^*}{(\gamma - 1)\rho_L^*} \ , \tag{12}$$

and estimates for the local speed of sound (for later use in the interpolation of the interface properties) are

$$a_L^* = \sqrt{\gamma(\gamma - 1)e_L^*} \ . \tag{13}$$

The velocity of the wave (relative to the initial left state) is given by

$$u_L - ws_L = \left[\frac{\gamma + 1}{2}\frac{P_L}{\rho_L}\left(\frac{P^*}{P_L} + \frac{\gamma - 1}{\gamma + 1}\right)\right]^{1/2} \tag{14}$$

where ws_L is the velocity of the wave relative to the cell boundaries.

If the pressure falls across the left-moving wave (i.e. $P^* \leq P_L$), the isentropic-wave relations are used to obtain the intermediate properties. The local speed of sound is obtained from the Riemann invariant as

$$a_L^* = (\overline{U}_L - u_L^*)(\gamma - 1)/2 \ , \tag{15}$$

while the specific internal energy is obtained from the sound-speed relation as

$$e_L^* = \frac{(a_L^*)^2}{(\gamma - 1)\gamma} \ . \tag{16}$$

The density is obtained from the equation of state as

$$\rho_L^* = \frac{P^*}{(\gamma - 1)e_L^*} \tag{17}$$

and the velocity of the leading-edge of the wave (relative to the initial left state) is given by

$$u_L - ws_L = a_L \, . \tag{18}$$

3 Test Cases

3.1 High Mach Number Flow around a Sphere.

The robustness of the code is demonstrated by computing a Mach 60 flow over a $7.5mm$ radius sphere with a domain consisting of a 60×60 mesh of cells. The $y = 0$ boundary is the symmetry line (and stagnation line) while a tangency condition is applied at the surface of the sphere. Free-stream conditions of

$$\rho = 0.5097 \times 10^{-2} \ kg/m^3, \quad P = 427.1 \ Pa, \quad e = 2.095 \times 10^5 \ J/kg,$$

$$u = 20600\ m/s, \quad v = 0, \quad M_{nominal} = 60.1$$

are applied to the curved inflow boundary, the shape of which is derived from the shock-position correlations in [9]. Flow conditions at the outflow boundary are obtained by zero-order (constant) extrapolation. Initial conditions throughout the domain are set to

$$\rho = 0.5097 \times 10^{-2}\ kg/m^3, \quad P = 427.1\ Pa, \quad e = 2.095 \times 10^5\ J/kg, \quad u = 0, \quad v = 0.$$

Despite the very high temperatures in the shock layer, the gas is considered perfect with

$$\gamma = 1.4, \quad R = 287\ J/kg/K, \quad Pr = 0.72,$$

and Sutherland's law is used for the coefficient of viscosity. The Navier-Stokes equations are then integrated forward in time using high-order MUSCL interpolation and Euler time-stepping with a CFL number of 0.5.

Figure 2 shows the flow field (pressure and Mach contours) at $t = 13.6\mu s$ after the flow has approached steady state. Discrete points from experimentally derived correlations [9] are plotted on the pressure contours. Given that $M = 60$ is beyond the range of the data used for the correlations, agreement is good. The largest deviations are near the outflow boundary. Profiles of density and pressure along the line of cells adjacent to the x-axis are shown in Fig. 3. The shock appears to be captured in 2 or 3 cells with no oscillation and the density jump is close to the ideal strong-shock value of 6. The pressure ratio from free-stream to the stagnation point is 4621 which is very close to the ideal value of 4636 for $M = 60$ (see e.g. [8] Table II).

A similar calculation with $M = 12$ was reported in [1] and, for that condition, an Osher-type solver (i.e. stages 1 and 3 only) failed to produce a solution. Also, a finite-difference scheme using Roe-type flux-difference splitting required a rather large value for its entropy-fix parameter in order to obtain a physically reasonable solution (J. White, NASA Langley Research Centre, private communication). Also note that, while the $M = 60$ shock is very strong, the high temperature in the region behind the shock enhances the viscous dissipation and may result in a smoother solution than seen at lower Mach numbers.

3.2 Flow Over a Sharp Cone

To illustrate the behaviour of the solver in the presence of strong viscous effects, we show the computed results for $M \simeq 8$ flow over a sharp 7^o cone. The axis of the cone is aligned with the free stream.

Two cases are considered in which the cone flow domain is discretized as a set of 100×60 cells and 100×90 cells. Free-stream conditions of

$$\rho = 1.0809 \times 10^{-2}\ kg/m^3, \quad P = 165.51\ Pa, \quad e = 3.8281 \times 10^4\ J/kg,$$

$$T = 53.35\ K, \quad u = 1164.0\ m/s, \quad v = 0, \quad M_{nominal} = 7.95$$

are applied to the left and upper boundaries while the outflow boundary conditions are obtained by extrapolation and the cone surface is modelled as a no-slip, adiabatic boundary. To match the experimental conditions in [10], the gas was considered to be a perfect gas with

$$\gamma = 1.4, \quad R = 287\ J/kg/K, \quad Pr = 0.7,$$

and viscosity was obtained from the Sutherland expression

$$\mu = 1.611 \times 10^{-6} \frac{T^{3/2}}{T + 110.33}\ Pa.s\ .$$

Based on free-stream conditions and the length of the cone, the Reynolds is approximately 3.3×10^6. The initial state of the flow in the domain is

$$\rho = 1.0809 \times 10^{-2}\ kg/m^3, \quad P = 165.51\ Pa, \quad e = 3.8281 \times 10^4\ J/kg, \quad u = 0, \quad v = 0.$$

The Navier-Stokes equations are then integrated forward in time using high-order MUSCL interpolation and Euler time-stepping with a CFL number of 0.5.

Figure 4 shows the flow field (pressure and density contours) $t = 22ms$ after the flow has approached steady state. The pressure field is almost conically symmetric, as per the inviscid solution of Taylor and Macoll [11] (see also [12] Ch. 10) and the shock angle is still approximately the inviscid value of 10.5^o ([8], Chart 4). The shock, however, is slightly curved near the apex of the cone. Boundary layer profiles of velocity and temperature at $x^* = 1.0m$ are shown in Fig. 5 for both the present finite-volume solutions and a boundary-layer solution using edge conditions of

$$\rho_e = 2.044 \times 10^{-2}\ kg/m^3, \quad P_e = 416.7\ Pa, \quad u_e^* = 1148.6\ m/s, \quad T_e = 71.04\ K.$$

There is good agreement between the present finite-volume solutions and the spectrally-accurate solution [13], especially near the cone surface. Although the outer region of the boundary layer is underresolved, (even for the 100×90 mesh) the finite-volume solutions appear to be converging to the spectral solution.

References

[1] P. A. Jacobs. Single-block Navier-Stokes integrator. ICASE Interim Report 18, 1991.

[2] J. J. Gottlieb and C. P. T. Groth. Assessment of Riemann solvers for unsteady one-dimensional inviscid flows of perfect gas. *Journal of Computational Physics*, 78(2):437–458, 1988.

[3] P. L. Roe. Approximate Riemann solvers, parameter vectors, and difference schemes. *Journal of Computational Physics*, 43:357–372, 1981.

[4] S. Osher and F. Solomon. Upwind difference schemes for hyperbolic systems of conservation laws. *Mathematics of Computation*, 38(158):339–374, 1982.

[5] J. J. Quirk. An adaptive grid algorithm for computational shock hydrodynamics. Ph.D. Thesis, Cranfield Institute of Technology, 1991.

[6] K. M. Peery and S. T. Imlay. Blunt-body flow simulations. AIAA Paper 88-2904, 1988.

[7] S. K. Godunov (Ed). *Numerical Solution of Multidimensional Problems in Gasdynamics.* Nauka, Moscow, 1976.

[8] Ames Research Staff. Equations, tables and charts for compressible flow. NACA Report 1135, 1953.

[9] F. S. Billig. Shock-wave shapes around spherical- and cylindrical-nosed bodies. *J. Spacecraft and Rockets*, 4(5):882–883, 1967.

[10] K. F. Stetson, E. R. Thompson, J. C. Donaldson, and L. G. Siler. Laminar boundary layer stability experiments on a cone at Mach 8. Part 1: Sharp cone. AIAA Paper 83-1761, 1983.

[11] G. I. Taylor and J. W. Maccoll. The air pressure on a cone moving at high speed. *Proc. Roy. Soc. (London) Ser. A*, 139:278–311, 1933.

[12] J. D. Anderson. *Modern Compressible Flow: with Historical Perspective.* McGraw-Hill, New York, 1982.

[13] C. D. Pruett and C. L. Street. A spectral collocation method for compressible, nonsimilar boundary layers. *Int. J. Num. Meth. Fluids*, Accepted for publication, 1991.

```
if (u* > 0) then

  The contact-discontinuity has moved to the right
  and the interface state is determined from the
  L and L* states.

  if (P* > P_L) then
    The left-moving wave is a shock.
    if (ws_L ≥ 0) then
      All waves have moved to the right.
      Interface state is equal to L.
    else
      Interface state is equal to L*.
    endif
  else
    The left-moving wave is a rarefaction.
    if (u_L - a_L ≥ 0) then
      All waves have moved to the right.
      Interface state is equal to L.
    elseif (u*_L - a*_L > 0) then
      The rarefaction straddles the interface.
      Interpolate the interface state from
      states L and L*.
    else
      The entire rarefaction moved to the
      left of the interface.
      Interface state is equal to L*.
    endif
  endif

else

  The contact discontinuity has moved to the left
  and the interface state is determined from the
  R and R* states in a similar manner...

endif
```

Figure 1: Interpolation logic for the Riemann solver.

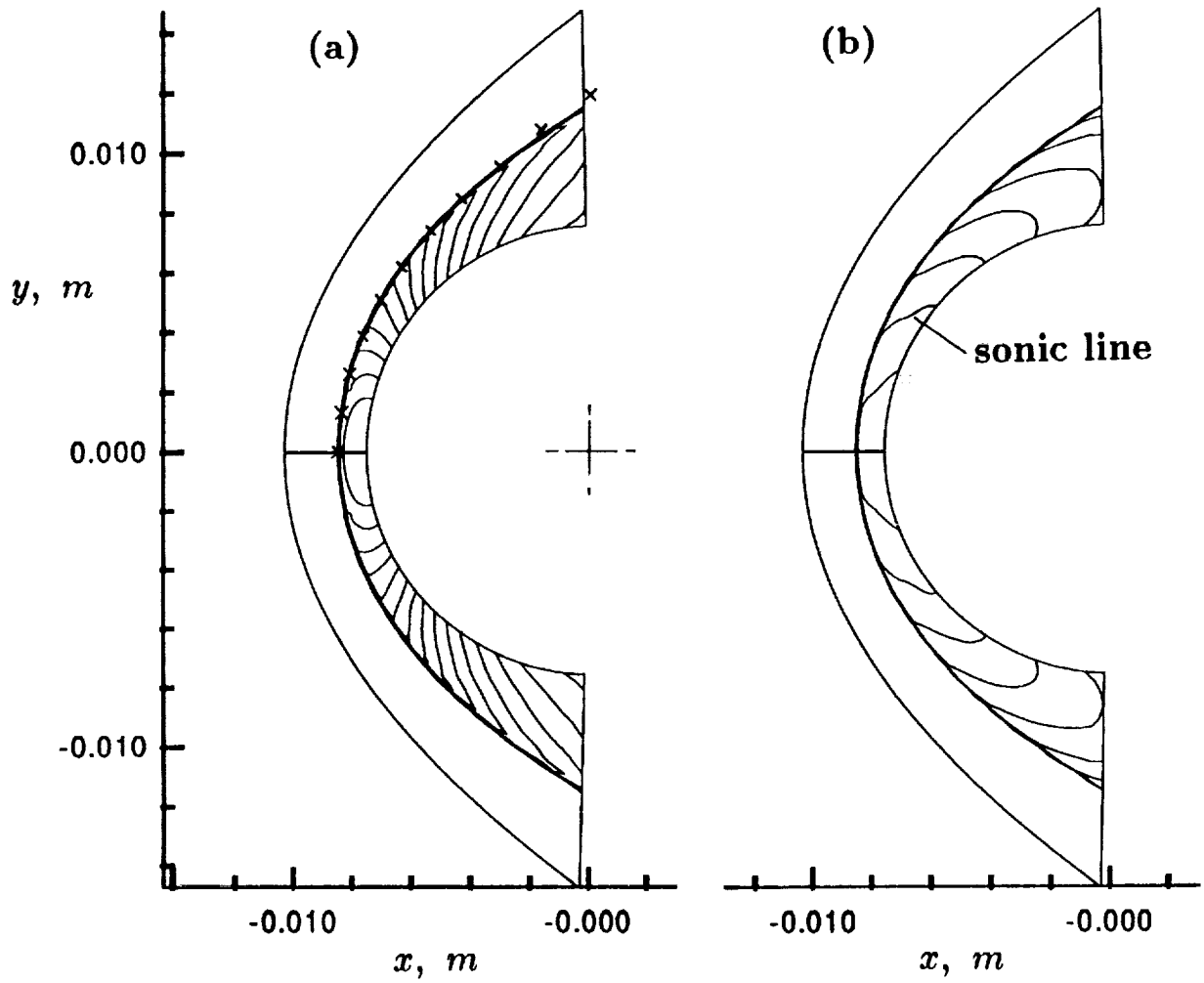

Figure 2: M = 60 flow over a sphere with a tangency boundary condition: (a) pressure contours; (b) Mach number contours. "+" denotes the experimental correlation.

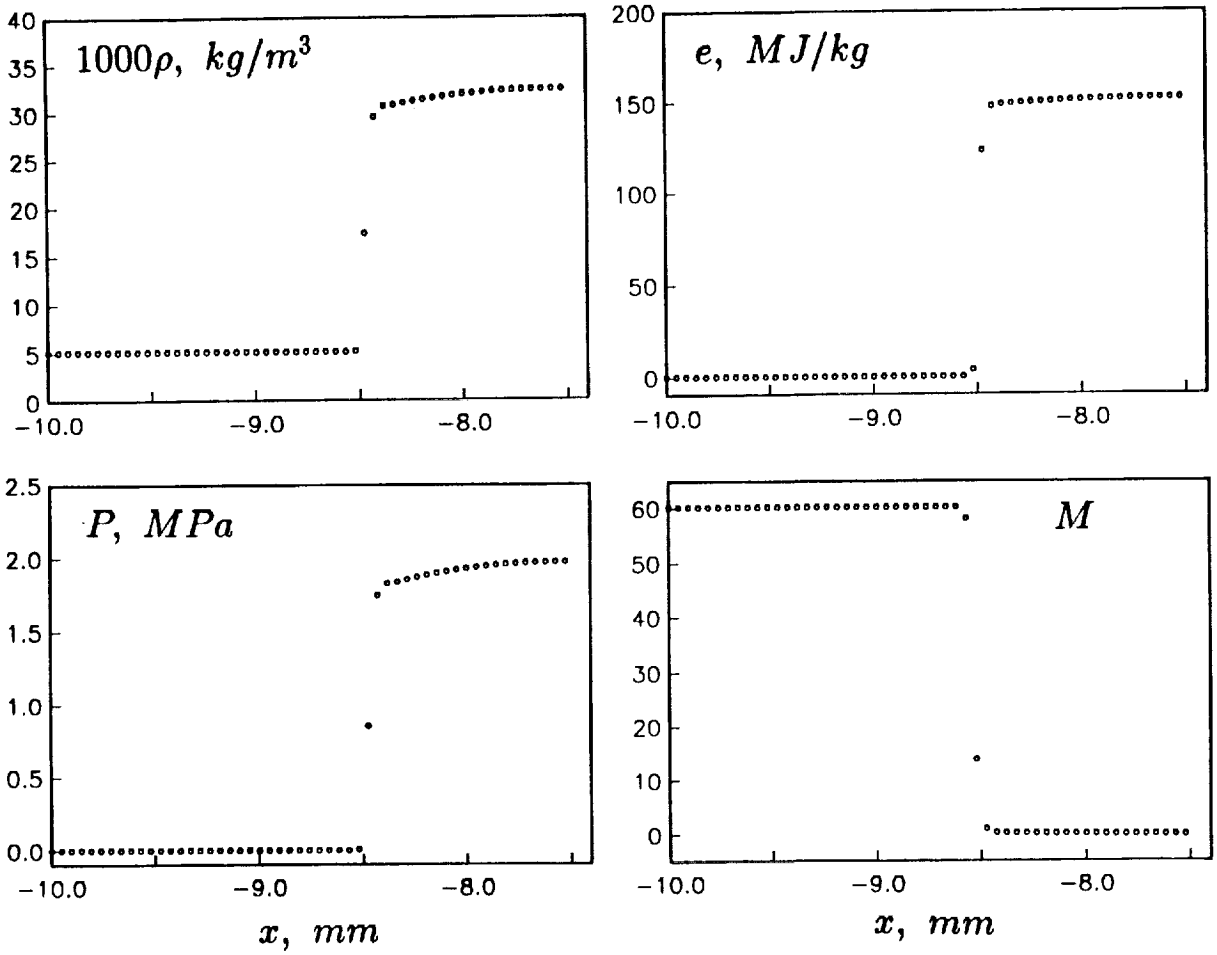

Figure 3: Flow properties for the cells adjacent to the ($y = 0$) stagnation line.

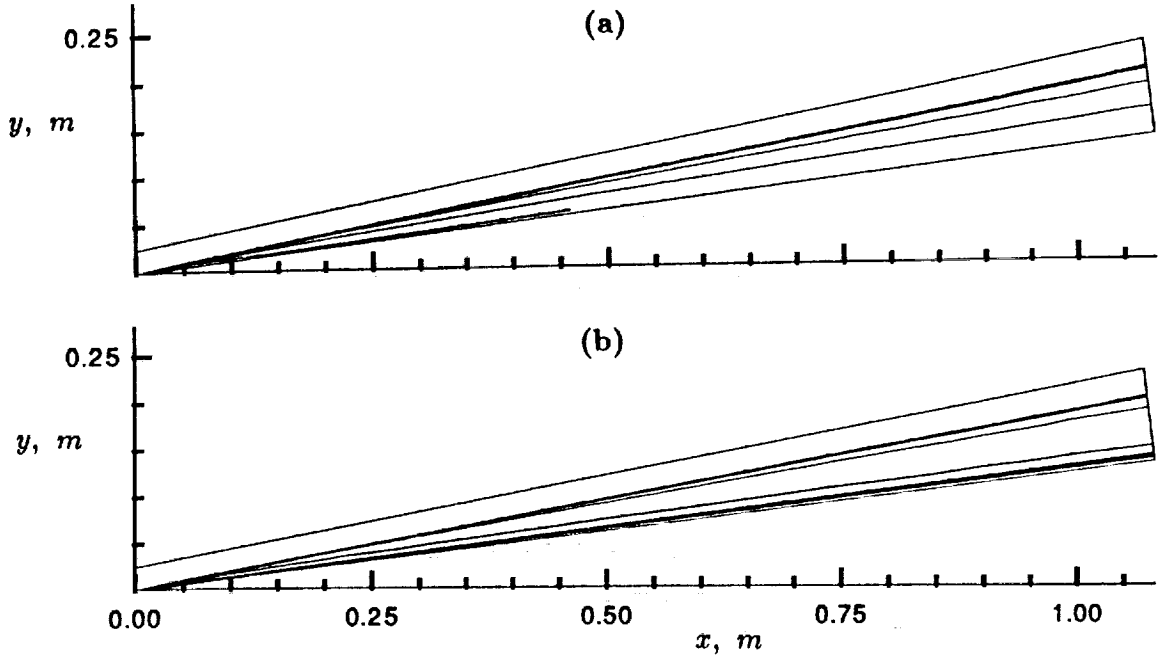

Figure 4: Flow over a 7° cone with an adiabatic boundary layer: (a) pressure contours; (b) density contours.

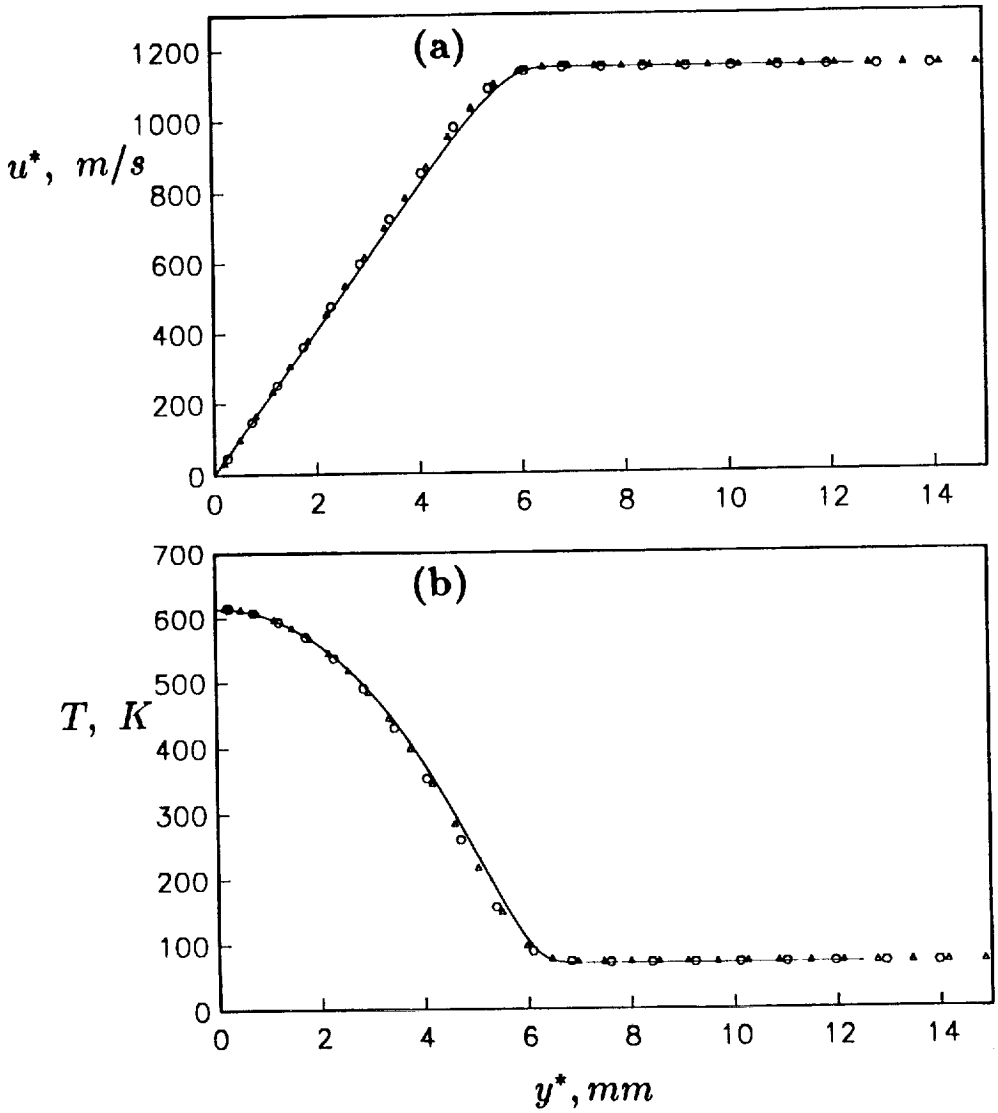

Figure 5: Comparison of the present finite-volume solution with a spectral solution at $1.0m$ from the cone apex: (a) tangential velocity; (b) temperature. Solid line represents spectral solution, ◯ denotes 100×60 mesh, △ denotes 100×90 mesh.

REPORT DOCUMENTATION PAGE

Form Approved
OMB No. 0704-0188

1. AGENCY USE ONLY (Leave blank)	2. REPORT DATE	3. REPORT TYPE AND DATES COVERED
	September 1991	Contractor Report

4. TITLE AND SUBTITLE
An Approximate Riemann Solver for Hypervelocity Flows

5. FUNDING NUMBERS
C NAS1-18605
WU 505-90-52-01

6. AUTHOR(S)
Peter A. Jacobs

7. PERFORMING ORGANIZATION NAME(S) AND ADDRESS(ES)
Institute for Computer Applications in Science and Engineering
Mail Stop 132C, NASA Langley Research Center
Hampton, VA 23665-5225

8. PERFORMING ORGANIZATION REPORT NUMBER
ICASE Report No. 91-75

9. SPONSORING/MONITORING AGENCY NAME(S) AND ADDRESS(ES)
National Aeronautics and Space Administration
Langley Research Center
Hampton, VA 23665-5225

10. SPONSORING/MONITORING AGENCY REPORT NUMBER
NASA CR-187629
ICASE Report No. 91-75

11. SUPPLEMENTARY NOTES
Langley Technical Monitor: Michael F. Card
Final Report
Submitted to AIAA Journal as "Technical Notes"

12a. DISTRIBUTION/AVAILABILITY STATEMENT
Unclassified - Unlimited

Subject Category 34

12b. DISTRIBUTION CODE

13. ABSTRACT *(Maximum 200 words)*

We describe an approximate Riemann solver for the computation of hypervelocity flows in which there are strong shocks and viscous interactions. The scheme has three stages, the first of which computes the intermediate states assuming isentropic waves. A second stage, based on the strong shock relations, may then be invoked if the pressure jump across either wave is large. The third stage interpolates the interface state from the two initial states and the intermediate states. The solver is used as part of a finite-volume code and is demonstrated on two test cases. The first is a high Mach number flow over a sphere while the second is a flow over a slender cone with an adiabatic boundary layer. In both cases the solver performs well.

14. SUBJECT TERMS
Riemann solver; hypervelocity flow

15. NUMBER OF PAGES
15

16. PRICE CODE
A03

17. SECURITY CLASSIFICATION OF REPORT	18. SECURITY CLASSIFICATION OF THIS PAGE	19. SECURITY CLASSIFICATION OF ABSTRACT	20. LIMITATION OF ABSTRACT
Unclassified	Unclassified		

NSN 7540-01-280-5500

Standard Form 298 (Rev 2-89)
Prescribed by ANSI Std Z39-18
298-102

NASA-Langley, 1991